Analytical Solution of Paraglide Wing Canopy Cell

[1]Md. Hasanuzzam and [2]Mohammad Mashud
[1]Department of Mathematics
[2]Department of Mechanical Engineering
Khulna University of Engineering & Technology
KUET, Khulna-9203, Bangladesh.
E-mail: mdmashud@yahoo.com

ABSTRACT

Aircraft recovery is possible using an inflatable wing canopy with steel cable or fiber suspension lines. These lines are attached to reels at the aircraft that not only provide stowage for the lines but braking during deployment to prevent high snatch forces. They can vary the inflated wings angle attack thereby controlling range and flared landing maneuver. The inflated pressurized wing can carry a larger load than flexible gliding parachutes. A combined aerodynamic-structural analysis is made which is based on the assumption that the sail is flexible and has freedom to make the shape which the aerodynamic pressure and the internal stresses dictate. Analytical results are obtained for Newtonian impact aerodynamic theory and are compared with results obtained for a rigid idealization of the paraglider wing. The calculations provide a basis for design of paragliders for hypersonic flight.

Nomenclature

L	lift
D	Drag
V	Free stream velocity
ρ	Free stream density
q	Dynamic pressure
S	Aerodynamic surface
α	Angle of attack
C	Chord length
C_L	Coefficient of lift
C_D	Coefficient of Drag
AR	Aspect ratio
I_L	Length of leading-edge boom
I_K	Length of keel boom
F_L	Force acting on leading-edge boom
F_K	Force acting on keel boom

Keywords: *Inflatable wing, Paraglide, Analytical Solution etc.*

1. Introduction

An inflatable wing aircraft recovery system that can be packed like parachute, deployed during an emergency, and is light enough in weight to be a practical recovery device for current aircraft designs.

In this case a theoretical investigation is made which consists of a combined structural and aerodynamic analysis. In this analysis, the sail is assumed to be an in extensional, flexible membrane which has complete freedom to take the shape which the aerodynamic pressures and the internal stresses dictate. The assumptions are also made that the booms are rigid and straight and that they have small enough cross sections so as not to affect the aerodynamics. The boom are maintained a fixed distance apart by spreader bars, and the dihedral of the leading-edge booms is fixed with respect to the keel boom.

The aerodynamic theory used is Newtonian theory, which has sometimes been used to express the aerodynamic pressure-shape relationship for the hypersonic speed range. Numerical results are presented to show effects of variation in dihedral angle (raising or lowering of the leading-edge booms).

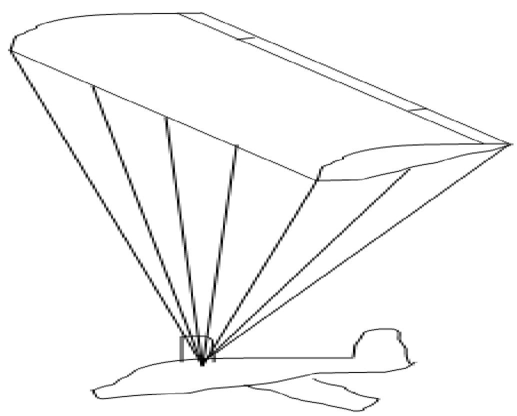

Fig: Aircraft Recovery System, RESCUE

2. Mathematical Analysis

2.1 Geometry of the sail

In this analysis the sail is assumed to be constructed from a flat, in extensional membrane which may take some rather general shape in its loaded equilibrium condition. By virtue of its inextensibility, it is possible to establish appropriate coordinates in the surface by considering the sail in its flat (unloaded) condition. (See fig.2 (a.)) Points on the sail are thus designated by the coordinates x and θ. Since the paraglider wing is symmetric about the x_1 axis(fig. 1), and since only symmetric deformations and loadings will be considered herein, only that portion of the wing in the first quadrant need be considered. The keel boom, of length l_k ,$0$is located at $0 - 0$ and the leading edge boom, of length l_K at $\theta = \theta_L$. It is also assumed that the trailing edge of the sail is straight; points on the trailing edge are expressed by the equation

$$X_T = \frac{l_K A}{\sin\theta + A\cos\theta} \tag{1}$$

Where

$$A = \frac{\sin\theta_L}{\frac{l_K}{l_L} - \cos\theta_L} \tag{2}$$

And a subscript T has been added to indicate that the values of x from this equation are values at the trailing edge.

For the x,θ polar coordinate system, the first fundamental form is given by

$$ds^2 = dx^2 + x^2 d\theta^2 \tag{3}$$

Since the booms are straight and rigid and lie on x-coordinate lines and since deformations of the sail are assumed in extensional, the x,θ coordinate curves are lines of principal curvature of the loaded surface for which

$$R_2 = \frac{x^2}{g}, \quad R_1 = \infty \tag{4}$$

are the radii of principal curvature. This is a surface of zero Gaussian curvature which has the second fundamental form g$d\theta^2$. Note that the sign convention on g differs from that usually employed in references in differential geometry of surfaces in that, for positive curvature of the surface, the positive direction of the normal is outward. The only one of the codazzi equations of compatibility (see [11]) not identically satisfied becomes

$$\frac{\partial g}{\partial x} = \frac{g}{x}$$

Integration of equation (5) yields

$$g = \frac{x}{R(\theta)} \tag{6}$$

Where R (θ) is an arbitrary function of θ alone. Then the radius of curvature R_2(eq. (4)) is

$$R_2 = XR(\theta) \tag{7}$$

2.2 Equilibrium Equations

Equilibrium of the loaded sail is governed by the equilibrium equations of membrane of zero Gaussian curvature (see, for example, [12]). In terms of the x,θ coordinates, these are:

$$xN_{x,x} + N_{x\theta,\theta} + N_X - N_\theta = 0 \tag{8}$$

$$xN_{X\theta,X} + N_{\theta,\theta} + 2N_{X\theta} = 0 \tag{9}$$

$$N_\theta = R_2 X = X(RX) \tag{10}$$

For the case where only normal pressure forces x act on the surface of the sail. Here N_X and N_θ are the normal stress resultants in the x and θ directions, respectively, and $N_{X\theta}$ is the shearing stress resultant. The comma followed by a subscript denotes partial differentiation with respect to this subscript.

2.3 Boundary Conditions

It is appropriate to consider force boundary conditions along a general boundary contour c of the loaded surface. Thus, one may prescribe

$$P_L = l_1^2 + 2l_1l_2N_{X\theta} + l_2^2N_\theta \qquad (11)$$
$$P_S = l_1S_1N_X + (l_1s_2 + l_2s_1)N_{X\theta} + l_2s_2N_\theta$$

Where P_L and P_S are applied boundary forces per unit length in the surface normal and tangent to c, respectively. Here l_1 and l_2 are the components of the unit outward surface normal $\bar{L}$ to c and s_1 and s_2 are components of the unit tangent $\bar{S}$ (in the direction of increasing $\bar{S}$). Since $\bar{L}$ and $\bar{S}$ are orthogonal vectors

$$s_1l_1 + s_2l_2 = 0 \qquad (12)$$
$$s_1^2 + s_2^2 = 1 \qquad (13)$$
$$l_1^2 + l_2^2 = 1 \qquad (14)$$

From figure 3 it can be seen that

$$s_1 = \frac{dX}{ds} \qquad (15)$$
$$s_2 = X\frac{d\theta}{ds}$$

For a given boundary contour c, s_1 and s_2 can be found from equations (13) and (15) and l_1 and l_2 form equations (12) and (14). Then the force boundary conditions for the given contour are determined from equations (11).

2.3.1 Trailing-edge boundary conditions

At the trailing edge the boundary contour is expressed by equation (1). From equations (1) and (15) the following is obtained:

$$(\sin\theta + A\cos\theta)s_1 + (\cos\theta - A\sin\theta)s_2 = 0 \qquad (16)$$

Simultaneous solution of equations (13) and (16) together with the solution of equations (12) and (14) yields

$$s_1 = -l_2 = -\frac{1}{\sqrt{1+A^2}}(\cos\theta - A\sin\theta) \qquad (17)$$

$$s_2 = -l_1 = -\frac{1}{\sqrt{1+A^2}}(\sin\theta + A\cos\theta) \qquad (18)$$

Now application of equation (11) along a stress-free trailing edge yields

$$(P_L)_T = \frac{1}{1+A^2}[(\sin\theta + A\cos\theta)^2 (N_{X\theta})_T$$
$$+2(\cos\theta - A\sin\theta)(\sin\theta + A\cos\theta)(N_{X\theta})_T$$
$$+(\cos\vartheta - A\sin\theta)^2 (N_{X\theta})_T = 0 \quad (19)$$

And

$$(P_S)_T = \frac{1}{1+A^2}\{(\sin\theta + A\cos\theta)(\cos\theta - A\sin\theta)[(N_\theta)_T$$
$$-(N_X) + [(\sin\theta + A\cos\theta)^2 - (\cos\theta - A\sin\theta)^2](N_{X\theta})_T\} \quad (20)$$

Finally, equations (19) and (20) may be recast in convenient form by solving for $(N_{X\theta})_T$ and $(N_X)_T$ and using equations (1) and (10)

$$(N_{X\theta})_T = \left(\frac{dX_T}{d\theta}\right)(RX)_T \quad (21)$$

And

$$(N_X)_T = \frac{1}{X_T}\left(\frac{dX_T}{d\theta}\right)^2 (RX)_{T\xi} \quad (22)$$

2.3.2 Nose boundary conditions

The boundary conditions at the nose of the sail are obtained by considering the limiting case of a stress-free boundary that shrinks to a point. Hence the stress resultants N_X , N_θ, and $N_{X\theta}$ must remain finite at this point.

2.3.3 Keel and leading-edge boundary conditions

The boundary conditions at the keel and leading edge are given by specifying the relative positions of the keel and leading edge. Details of the specification of these boundary conditions are reserved to a subsequent section.

2.4 Solution of Equilibrium Equations

Substitution of the expression for N_θ from equation (10) into equations (8) and (9) yields

$$(xN_X)_{,X} \mid N_{X\theta,\theta} = X(RX) \quad (23)$$

$$(X^2 N_X)_{,X} = -X^2 (RX)_{,\theta} \quad (24)$$

Integration of equation (24) gives

$$N_{\theta X} = -\frac{1}{X^2}\int_0^X \xi^2 (RX)_{,\theta} d\xi \quad (25)$$

Where the boundary condition for finiteness of the stress resultant at the nose of the sail has been satisfied. Substitution of $N_{X\theta}$ from equation (25) into equation (25) and integration then yields

$$N_X = \frac{1}{X}\int_0^X [\xi(RX) + \frac{1}{\xi^2}\int_0^\xi \lambda^2 (RX)_{,\theta\theta} d\lambda] d\xi \quad (26)$$

Where again, the boundary condition at x=0 has been imposed. Thus, the stress resultants N_{θ}, $N_{X\theta}$ and N_X are readily expressed in terms of the aerodynamic pressure X(X, θ) and the single parameter R(θ).

Now the boundary conditions (21) and (22) for stress resultants at the trailing edge of the sail are seen to require:

$$-\frac{1}{X_T^2}\int_0^{X_T} \xi^2 (RX)_{,\theta} d\xi = \left(\frac{dX_T}{d\theta}\right)(RX)_T \tag{27}$$

$$\frac{1}{X_T}\int_0^{X_T}\left[\xi(RX) + \frac{1}{\xi^2}\int_0^{\xi}\lambda^2 (RX)_{,\theta\theta} d\lambda\right] d\xi = \frac{1}{X_T}\left(\frac{dX_T}{d\theta}\right)^2 (RX)_T \tag{28}$$

T should be noted that both equations (27) and (28) must be satisfied. However, only the one arbitrary function R(θ) is available for satisfying these woe conditions. Difficulties of this nature are commonly found when dealing with membrane shells of zero Gaussian curvature (see, for example, [12]) and as a result membrane stress states can, in general, be obtained only in special cases. For the straight trailing-edge boundary conditions considered in this problem the fortunate situation arises that, for any aerodynamic pressures of the type

$$X(X.\theta) = \sum_{m=-1}^{\infty} a_n X^n Z_n(\theta) \tag{29}$$

a single function R(θ) can be found which satisfies both equations (27) and (28) and thus leads to true membrane stress states. Moreover, for aerodynamic pressures of this type, a straight trailing edge is necessary for obtaining a membrane stress state satisfies both trailing-edge boundary conditions.

The parameter R(θ) expresses the shape of the loaded surface of the sail and the aerodynamic pressure X(X, θ) is dependent on this shape. It is convenient for deriving a relationship between aerodynamic loading and the shape to express the shape in terms of angles β(θ) and δ(θ) measured from the keel location rather than by R(θ) .(See fig. 2(b).) In appendix A the parameter R(θ)δ is found in terms of β and δ is related to β via the condition of inextensibility. The resulting equations are

$$R(\theta) = \frac{-\sqrt{1-(\frac{d\beta}{d\theta})^2}}{\frac{d^2\beta}{d\theta^2}+\frac{\sin\beta}{\cos\beta}\left[1-(\frac{d\beta}{d\theta})^2\right]} \tag{30}$$

And

$$\frac{d\delta}{d\theta} = \pm\frac{1}{\cos\beta}\sqrt{1-\left(\frac{d\beta}{d\theta}\right)^2} \tag{31}$$

2.5 Application of Newtonian Impact Theory

The entire analysis up to this point is based upon equilibrium consideration of the sail subjected to normal pressure, and the equations derived are not dependent upon any specific aerodynamic theory. In this section use is made of Newtonian impact theory. (see, for example, [9,10].) This theory, often used for hypersonic velocities, has the advantage of yielding pressures X which are functions of θ alone and thus permitting satisfaction of the boundary conditions (27) and (28). In addition, this aerodynamic theory has also been applied in [7] to a rigid idealization of a paraglide

wing; therefore, a direct comparison can be made with the results of [7] to evaluate the use of rigid models in the study of paraglide behavior.
In Newtonian impact theory, the pressure at a point is given by the relation

$$X = 2q\sin^2 \epsilon \quad \text{if } \epsilon \geq 0$$
Or (32)
$$X = 0 \quad if \ \epsilon < 0$$

Where q is the dynamic pressure and ε is the angle between the local stream wise unit tangent vector and the free-stream velocity vector. Newtonian impact theory requires that the moving stream gives up its "normal" component of momentum (to the surface impact) but retains the tangential component which passes off tangentially to the local surface. Only portions of the surface that "see" the flow have a nonzero pressure coefficient, as indicated in equations (32).The unit normal $\bar{V}$ to the surface has been determined in terms of the parameters β and δ in appendix A(see eq.(52)). If it is noted that sin ϵ =cos($\bar{\iota}$,$\bar{v}$)=$\bar{\iota}$. $\bar{v}$, and is made of equations (52), the pressure on the sail at a given point (eq.(32)) is readily expressed as

$$X = 2q[(\cos\beta \sin\alpha - \sin\beta\cos\delta\cos\alpha)\sqrt{1-(\frac{d\beta}{d\theta})^2}+\sin\delta\cos\propto\frac{d\beta}{d\theta}]^2 \tag{33}$$

From equation (33), it is evident that X is a function of θ alone. For this case, the boundary conditions (27) and (28) on the stress resultants at the trailing edge of sail are satisfied by

$$(RX)=\frac{C}{X_T^3} \tag{34}$$

Here the constant of integration C is to be determined by the relative positions of the keel and leadings edge.

Equation (34) upon substitution from equation (33) for X and equation (30) for R yields a differential equation from which the deflected shape of the sail is determined ;thus

$$-\sqrt{1-(\frac{d\beta}{d\theta})^2}[\cos\beta\sin\alpha - \sin\beta\cos\delta\cos\alpha)\sqrt{1-(\frac{d\beta}{d\theta})^2}+\cos\alpha\sin\delta\frac{d\beta}{d\theta}]^2$$
$$=\frac{1}{2}(\frac{C}{q l_k^3}(\frac{1}{A}\sin\theta+\cos\theta)^3\left\{\frac{d^2\beta}{d\theta^2}+\frac{\sin\beta}{\cos\beta}\left[1-\left(\frac{d\beta}{d\theta}\right)\right]\right\} \tag{35}$$

One other relation is needed. This is provided by integration of equation (31):

$$\delta = \int_0^{\theta}\frac{1}{\cos\beta}\sqrt{1-(\frac{d\beta}{d\theta})^2}d\theta \tag{36}$$

The negative sign in equation (31) is ruled out since the lower (or upstream) surface must "see" the flow. Solution of the simultaneous nonlinear equations (35) and (36), for β and δ, and satisfaction of specified conditions $\beta(\theta_L)$ and $\delta(\theta_L)$, at the leading edge of the sail , determines the deflected shape of the sail . This solution is affected by using finite differences to represent derivatives of β with respect to θ:

$$\left(\frac{d\beta}{d\theta}\right)_n=\frac{1}{2\Delta}(\beta_{n+1}-\beta_{n-1})$$
$$\left(\frac{d^2\beta}{d\theta^2}\right)_n=\frac{1}{\Delta^2}(\beta_{n+1}-2\beta_n+\beta_{n-1}) \tag{37}$$

Where Δ is the spacing of the stations and station n=0 is taken at the keel. Parabolic integration is employed to evaluate the integral in equation (36) so that

$$\delta_n=\delta_{n-1}+\frac{\Delta}{12}(5f_n+8f_{n-1}-f_{n-2}) \tag{38}$$

Where $$f_n=\frac{1}{\cos\beta_n}\sqrt{1-\left(\frac{d\beta}{d\theta}\right)_n^2}$$

Then , if values of $(d\beta/d\theta)_0$,(c/ql_k^3) ,and angle of attack α are specified ,equations (35) and (36) became two simultaneous equations for determining δ_n and β_{n+1} in terms of their values at preceding stations. For each set of selected values of $(d\beta/d\theta)_0$,(c/ql_k^3) , and α , these equations are applied successively to obtain a set of values of $\beta(\theta_L)$ and $\delta(\theta_L)$ at the leading edge. The values of $(d\beta/d\theta)_0$ and (c/ql_k^3) are then varied until the deflected shape with the desired boundary values of $\beta(\theta_L)$ and $\delta(\theta_L)$ is obtained.

The stress resultants may now be evaluated. With the relations (34) for RX, and (1) for X_T equations (10), (25) and (26) become

$$N_\theta=\left(\frac{c}{ql_k^3}\right)\frac{Xq}{A^3}(\sin\theta+A\cos\theta)^3$$
$$N_X=\left(\frac{c}{ql_k^3}\right)\frac{Xq}{A^3}(\sin\theta+A\cos\theta)(\cos\theta-A\sin\theta)^2 \tag{39}$$
$$N_{X\theta}=-\left(\frac{c}{ql_k^3}\right)\frac{Xq}{A^3}(\sin\theta+A\cos\theta)(\cos\theta-A\sin\theta)$$

Where A is given by equation (2) and where (c/ql_k^3) has been determined in the course of the numerical integration described above.

Determination of the two principal stress resultants yields the value zero and

$$N=\left(\frac{c}{ql_k^3}\right)\frac{Xq}{A^3}(1+A^2)(\sin\theta+A\cos\theta) \tag{40}$$

Acting perpendicular and parallel to the trailing edge, respectively. From figure 2(a) and equation (1) it can be seen that lines parallel to the trailing edge are given by

$$X=\frac{(X)_{\theta=0}A}{\sin\theta+\cos\theta} \tag{41}$$

So that along these lines the maximum principal stress resultant is a constant:

$$N = \frac{c}{q l_K^2} \frac{(X)_{\theta=0} q}{A^2} (1+A^2) \tag{42}$$

Integration of the stress resultants given by equations (39) at the keel and leading edge yields the resultant forces applied by the sail to the booms. (See fig 4.) Then by considering the components of the boom forces in the z_0 and x_0 directions, the lift and the drag forces are obtained. The boom forces and the lift and drag forces are determined in appendix B.

2.5 Shape of Loaded Surface of the Sail

In this appendix the shape of the loaded surface of the sail is presented by the angles β and δ shown in figure 2(b). The X_1- axis of the rectangular Cartesian coordinates X_1,Y_1,Z_1 is alined with the keel of the paraglide and the X_1Z_1 plane is the vertical plane of symmetry of the paraglide. Hence

$$\left.\begin{aligned} Z_1 &= X \sin\beta \\ X_1 &= X \cos\beta \cos\delta \\ y_1 &= X \cos\beta \sin\delta \end{aligned}\right| \tag{43}$$

Consider the keel at an angle of attack α and define rectangular Cartesian coordinates x_0, y_0, z_0 such that the x_0- axis is aliened with the direction of airflow. The x_0z_0- plane is coincident with the x_1z_1- plane (fig.1), thus

$$\left.\begin{aligned} Z_0 &= X(\sin\beta\cos\alpha - \cos\beta\cos\delta\sin\alpha) \\ X_0 &= X(\sin\beta\sin\alpha + \cos\beta\cos\delta\cos\alpha) \\ y_0 &= X\cos\beta\sin\delta \end{aligned}\right| \tag{44}$$

Now if z_0 is treated as a function of x_0 ,y_0 representing the deflected surface in the x_0 ,y_0 ,z_0 coordinate system,

$$dZ_0 = \frac{\partial Z_0}{\partial X_0} dX_0 + \frac{\partial Z_0}{\partial y_0} dy_0 \tag{45}$$

And it can be shown from equations (44) and (45) that:

$$\frac{\partial Z_0}{\partial X_0} = \frac{-\sin\delta\cos\alpha\frac{d\beta}{d\theta} + (\sin\beta\cos\delta\cos\alpha - \cos\beta\sin\alpha)\cos\beta\frac{d\delta}{d\theta}}{-\sin\delta\sin\alpha\frac{d\beta}{d\theta} + (\sin\beta\cos\delta\sin\alpha + \cos\beta\cos\alpha)\cos\beta\frac{d\delta}{d\theta}} \tag{46}$$

And

$$\frac{\partial Z_0}{\partial y_0} = \frac{\cos\delta\frac{d\beta}{d\theta} + \sin\beta\cos\beta\sin\delta\frac{d\delta}{d\theta}}{-\sin\delta\sin\alpha\frac{d\beta}{d\theta} + (\sin\beta\cos\delta\sin\alpha + \cos\beta\cos\alpha)\cos\beta\frac{d\delta}{d\theta}} \tag{47}$$

Also the square of the length of a line element on the deflected surface is given by

$$dS^2 = dX_0^2 + dy_0^2 + dZ_0^2 \quad (48)$$

Which upon substitution from equations (44) and (45) yields

$$dS^2 = dX^2 + X^2\left[\left(\frac{d\beta}{d\theta}\right)2 + COS^2\beta\left(\frac{d\beta}{d\theta}\right)2\right]d\theta^2 \quad (49)$$

But inextensibility requires that the metric (eq. (3)) remain unchanged; thus, it follows from equation (49) tat

$$\frac{d\delta}{d\theta} = \pm\frac{1}{\cos\beta}\sqrt{1-(\frac{d\beta}{d\theta})^2} \quad (50)$$

The unit outward normal of the deflected surface is given by

$$\bar{V} = \pm\frac{1}{\left[\left(\frac{\partial z_0}{\partial x_0}\right)^2+\left(\frac{\partial z_0}{\partial y_0}\right)^2+1\right]^{1/2}}\left[-\frac{\partial z_0}{\partial x_0}\bar{\iota}-\frac{\partial z_0}{\partial y_0}\bar{J}+\bar{k}\right] \quad (51)$$

Where the positive sign refers to surfaces which are concave downward, and the minus sign to those which are concave upward. The unit normal's $\bar{\iota}$,$\bar{J}$ and $\bar{k}$ are directed along the x_0^-, y_0^- and z_0^- axes as shown in figure 1. Upon substitution from equations (46),(47) and (50) for $\partial z_0/\partial x_0$, $\partial z_0/\partial y_0$ and $d\delta/d\theta$ equation (51) yields

$$\bar{v} = \left[(\cos\beta\sin\alpha - \sin\beta\cos\delta\cos\alpha)\sqrt{1-\left(\frac{d\beta}{d\theta}\right)2} + \sin\delta\cos\alpha\frac{d\beta}{d\theta}\right]\bar{\iota} - \left[\sin\beta\sin\delta\sqrt{1-\left(\frac{d\beta}{d\theta}\right)2} + \cos\delta\frac{d\beta}{d\theta}\right]\bar{J} + \left[\left(\cos\beta\cos\alpha + \sin\alpha\cos\delta\sin\alpha\sqrt{1-\left(\frac{d\beta}{d\theta}\right)2} - \sin\delta\sin\alpha\frac{d\beta}{d\theta}\right)\right]\bar{k} \quad (52)$$

The unit tangential vector in the x-direction is given by

$$\bar{T_1} = (\sin\beta\sin\alpha + \cos\beta\cos\delta\cos\alpha)\bar{\iota} + (\cos\beta\sin\delta)\bar{J} + (\sin\beta\cos\alpha - \cos\beta\cos\delta\sin\alpha)\bar{k} \quad (53)$$

The unit tangential vector in the θ-direction is given by

$$\bar{T_2} = \bar{v}\times\bar{T_1}$$

$$\left[\cos\delta\sqrt{1-(\frac{d\beta}{d\theta})^2}\sin\beta\sin\delta\frac{d\beta}{d\theta}\right]\bar{J} + \left[\sin\delta\sin\alpha\sqrt{1-(\frac{d\beta}{d\theta})^2} + (\cos\beta\cos\alpha + \sin\beta\cos\delta\sin\alpha)\frac{d\beta}{d\theta}\right]\bar{k} \quad (54)$$

The quantity g can be expressed in terms of $\bar{v}$ and $\bar{\tau}$ and then in terms of the angle β by using equations (52) and (54):

$$g = X\bar{T}_2.\bar{v},$$

$$g = \frac{-X}{\sqrt{1-(\frac{d\beta}{d\theta})^2}}\left\{\frac{\sin\beta}{\cos\beta}\frac{\sin\beta}{\cos\beta} + \frac{d^2\beta}{d\theta^2}\right\} \quad (55)$$

Then from equation (6) the function (θ) can be expressed in terms of the quantity β as

$$R(\theta) = \frac{-\sqrt{1-(\frac{d\beta}{d\theta})^2}}{\frac{d^2\beta}{d\theta^2}+\frac{\sin\beta}{\cos\beta}[1-(\frac{d\beta}{d\theta})^2]} \quad (56)$$

3. Calculation of Lift and Drag Forces on Paraglide Wing

In this section the lift and drag forces are derived. As a preliminary step, the resultant forces applied by the sail to the keel and leading edge booms are obtained. These resultant forces and their location are useful in obtaining the forces in the shroud lines and spreader bars of the paraglide.
The resultant force applied to the keel by the half of the sail considered in the analysis is obtained by integration of the stress resultants for the sail along the keel boundary. Since the tangent vectors along the keel do not vary with x the vector equation for the force is given by

$$\overline{F_K} = (\bar{T}_1)_K \int_0^{lK} N_{X\theta_{\theta=0}}\,dX + (\bar{T}_2)_K \int_0^{lK} N_{\theta_{\theta=0}}\,dX \quad (57)$$

And this force acts through the point $x=x_K$ of the keel, where

$$X_K = \frac{\int_0^{lK} XN_{X\theta_{\theta=0}}\,dX}{\int_0^{lK} N_{X\theta_{\theta=0}}\,dX} \quad (58)$$

Here $(\bar{\tau}_1)_k$ and $(\bar{\tau}_2)_k$ are the unit tangent vectors of the surface at the keel (eqs.(53) and (54) evaluated at θ=0). Similarly, the vector equation fro resultant force applied by the sail to the leading edge boom is given by

$$\overline{F_L} = (\bar{T}_1)_L \int_0^{lK} N_{X\theta_{\theta=\theta_L}}\,dX + (\bar{T}_2)_K \int_0^{lK} N_{\theta_{\theta=\theta_L}}\,dX \quad (59)$$

And this force acts through the point $x=x_L$ of the leading edge where

$$X_L = \frac{\int_0^{lK} XN_{X\theta_{\theta-\theta_L}}\,dX}{\int_0^{lK} N_{X\theta_{\theta=\theta_L}}\,dX} \quad (60)$$

In equation (59) $(\bar{\tau}_1)_L$ and $(\bar{\tau}_2)_L$ are the unit tangent vectors of the surface (eqs.(53) and (54)) at the leading edge $\theta=\theta_L$.

It is necessary now to determine the components of $\bar{F}_k$ and $\bar{F}_L$ in the x_0 ,y_0 and z_0 directions. For example, the component of $\bar{F}_k$ in the x_0 direction is given by

$$F_{KX_0} = \overline{F_K}.\bar{\iota} = \cos\alpha \int_0^{l_K} (N_{X\theta})_{\theta=0}\, dX + \sin\propto \left(\frac{d\beta}{d\theta}\right)_{\theta=0} \int_0^{l_K} (N_\theta)_{\theta=0}\, dX \qquad (61)$$

Or for Newtonian impact theory (eqn.(39)) in non dimensional form:

$$\frac{F_{KX_0}}{qS} = -\frac{1}{2}\left(\frac{C}{ql_K^2}\right)\frac{l_K/l_L}{\sin\theta_L}\left[\frac{1}{A}\cos\alpha - \left(\frac{d\beta}{d\theta}\right)_{\theta=0}\sin\alpha\right] \qquad (62)$$

Similarly the remaining components are

$$\frac{F_{Ky_0}}{qS} = \frac{1}{2}\left(\frac{C}{ql_K^2}\right)\frac{l_K/l_L}{\sin\theta_L}\sqrt{1-\left(\frac{d\beta}{d\theta}\right)^2_{\theta=0}} \qquad (63)$$

$$\frac{F_{KZ_0}}{qS} = \frac{1}{2}\left(\frac{C}{ql_K^2}\right)\frac{l_K/l_L}{\sin\theta_L}\left[\frac{1}{A}\sin\alpha + \left(\frac{d\beta}{d\theta}\right)\theta = 0 \quad \cos\propto\right] \qquad (64)$$

$$\frac{F_{LX_0}}{qS} = \frac{1}{2}\left(\frac{C}{ql_K^2}\right)\frac{(l_K/l_L)^2}{\sin\theta_L}\left(I_1\frac{\cos\theta_L - l_K/l_L}{\sin\theta_L} - I_2\right) \qquad (65)$$

$$\frac{F_{Ly_0}}{qS} = \frac{1}{2}\left(\frac{C}{ql_K^2}\right)\frac{(l_K/l_L)^2}{\sin\theta_L}\left(J_1\frac{\cos\theta_L - l_K/l_L}{\sin\theta_L} - J_2\right) \qquad (66)$$

$$\frac{F_{LZ_0}}{qS} = \frac{1}{2}\left(\frac{C}{ql_K^2}\right)\frac{(l_K/l_L)^2}{\sin\theta_L}\left(K_1\frac{\cos\theta_L - l_K/l_L}{\sin\theta_L} - K_2\right) \qquad (67)$$

Where

$$I_1 = \sin\beta(\theta_L)\sin\propto + \cos\beta(\theta_L)\cos\delta(\theta_L)\cos\propto \qquad (68)$$

$$J_1 = \cos\beta(\theta_L)\sin\delta(\theta_L) \qquad (69)$$

$$k_1 = \sin\beta(\theta_L)\cos\alpha - \cos\beta(\theta_L)\cos\delta(\theta_L)\sin\alpha \qquad (70)$$

$$I_2 = -\sin\delta(\theta_L)\cos\alpha\sqrt{1-\left(\frac{d\beta}{d\theta}\right)^2_{\theta=\theta_L}}$$
$$+[\cos\beta(\theta_L)\sin\alpha - \sin\beta(\theta_L)\cos\delta(\theta_L)\cos\alpha]\left(\frac{d\beta}{d\theta}\right)_{\theta=\theta_L} \qquad (71)$$

$$J_2 = \cos\delta(\theta_L)\sqrt{1-\left(\frac{d\beta}{d\theta}\right)^2_{\theta=\theta_L}} - \sin\beta(\theta_L)\sin\beta(\theta_L)\left(\frac{d\beta}{d\theta}\right)_{\theta=\theta_L}$$
$$+[\cos\beta(\theta_L)\cos\infty + \sin\beta(\theta_L)\cos\delta(\theta_L)\sin\infty]\left(\frac{d\beta}{d\theta}\right)_{\theta=\theta_L} \qquad (72)$$

$$k_2 = \sin\delta(\theta_L)\sin\infty\sqrt{1-\left(\frac{d\beta}{d\theta}\right)^2_{\theta=\theta_L}}$$
$$+[\cos\beta(\theta_L)\cos\infty + \sin\beta(\theta_L)\cos\delta(\theta_L)\sin\infty]\left(\frac{d\beta}{d\theta}\right)_{\theta=\theta_L} \qquad (73)$$

The coordinatesx_{OK}, etc. (fig. 4) through which these forces act may be written with the aid of equations (44), (58), and (60) as

$$x_{oL} = \frac{2}{3} l_K \cos \infty \tag{74}$$

$$y_{oL} = 0 \tag{75}$$

$$z_{QK} = -\frac{2}{3} l_K \sin \infty \tag{76}$$

$$x_{oL} = \frac{2}{3} l_L I_1 \tag{77}$$

$$y_{oL} = \frac{2}{3} l_L J_1 \tag{78}$$

$$z_{ol} = \frac{2}{3} l_L k_1 \tag{79}$$

Finally, when both haves of the symmetrical sail are considered (fig. 4), the lift and drag coefficients can be expressed as follows:

$$C_L = \frac{L}{qs} = \frac{2}{qs}(F_{KZ_O} + F_{LZ_O}) \tag{80}$$

$$C_D = \frac{D}{qs} = \frac{2}{qs}(F_{KX_O} + F_{LX_O}) \tag{81}$$

Where L and D are the lift and drag forces, respectively, on the wing; $q = \frac{1}{2}\rho V^2$ is the dynamic pressure, and

$$S = l_K l_L \sin \theta_L \tag{82}$$

Is the total surface area of the sail. The resultant of the lift and drag forces acts through the point $(\overline{X_O}, \overline{Z_O})$ where

$$\overline{X_O} = \frac{X_{OL} F_{LZO} + X_{OK} F_{KZO}}{F_{LZO} + F_{KZO}} \tag{83}$$

And

$$\overline{z_O} = \frac{z_{OL} F_{LXO} + Z_{OK} F_{KXO}}{F_{LXO} + F_{KX_O}} \tag{84}$$

4. Conclusion

Equilibrium equations for the sail of the paraglide wing have been derived and integrated. Results are first obtained in rather general form for the stress resultants in the sail, boom forces and lift and drag in terms of the pressure on the sail and a parameter that describes the deflected shape of the sail. The specification of an appropriate aerodynamic theory- in the present case, Newtonian impact theory- then permits satisfaction of the boundary conditions at the trailing edge and calculation of the deflected shape of the sail. Finally, the general formulas are applied to calculate the stress resultants, lift, and drag. Numerical results have been obtained and have been compared with published results for a rigid idealization of the paraglide wing. The comparison shows that the assumed shape of the rigid wing is considerably in error over the complete range of angles of attack. Consequently, the lift and coefficients and, especially the lift to drag ratio, for the flexible wing are significantly different from the values found for the rigid wing. The calculated stress resultants and boom forces provide a basis for design of sails, booms, shroud lines, and spreader bars for a paraglide in hypersonic flight.

References

[1]. U.S. Navy/Marine Corp. Aviation Accident Statistical Summary (1970), Confidential.

[2]. Low Cost Space Transportation System, North American Rockwell Corp., sp69-2, January 1969.

[3]. U.S. Air Force Stability and Control Methods, DATCOM, McDonnell Douglas Corp., September 1970

[4]. F-4 General Airframe Information, NAVAIR 01-245, Fob-2-1.1, April 1965.

[5]. Perry, D. J., Aircraft Structure, McGraw-Hill Book Co., Inc., 1950

[6]. Telephone conversation with Rodger H. Landolts, E.I. DuPont deNemours and Co. , Wilmington, Delaaware, February 12 , 1973.

[7]. Marks Mechanical Engineers Handbook, Sixth Edition, McGraw-Hill Book Co.

[8]. Orewer, N. W. and N. L. Jeppeson, “Methods of Evaluation of inflatable Structure for Space Applications”, Goodyear Aerospace Corp. , Akron, Ohio, NASA Contract NASW-471, N64-19370.

[9]. Thiokol Chemical Report EB-66, October 1966.

[10]. Forehand, J.E. and H. Q. Bair,”Parawing Precision Aerial Delivery Systems Conference, Volume 2, B1FTC-TR-69-11.

[11]. Coeller, J.H. and E. M. Linhart,”Parawing Technology for Spacecraft Land Landing” , A Progress Report , Northrop Corp. , Ventura Div. , Newbury Park , Cali . , AIAA Paper No. 70-1187

[12]. Hoerner, S. F. , “Fluid-Dynamic Drag” , published by author ,1958.

[13]. F-4J Performance Data and Sustention, McDonnell Douglas Corp. ,Report No. MDC-A1216, Vol. 1, July 15, 1971.

[14]. Eilertson, W.H. ,”Gliding Parachutes for Land Recovery” ,Bellcomm, Inc. ,Sept. 8, 1969,B69-09008.

[15]. Sleeman, W.C. and T.C. Gainer, ‘Status of Research on Para wing Lifting Decelerators”, NASA Langley Research Center, AIAA Paper No. 68-967.

[16]. Para Plane, Para Flit, Inc., Cherry Hill, New Jersey.

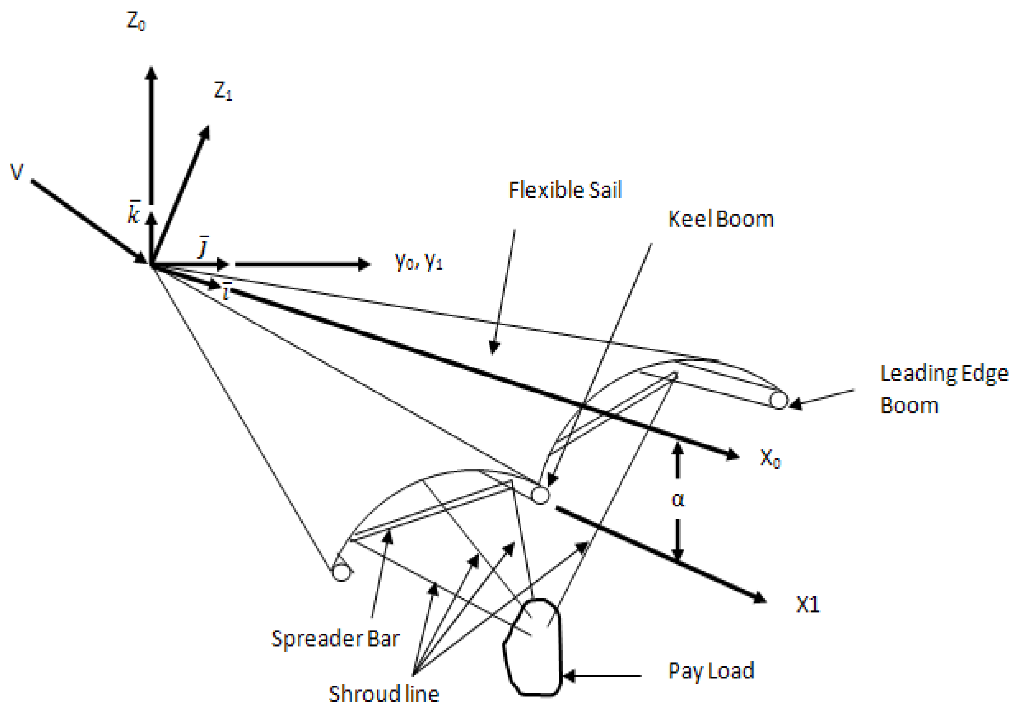

Fig 1: Para Glider Wing configuration

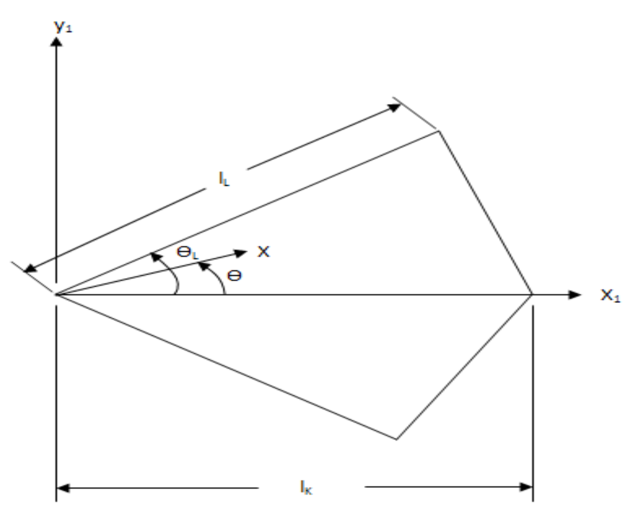

Fig 2(a):Co-ordinates of sail

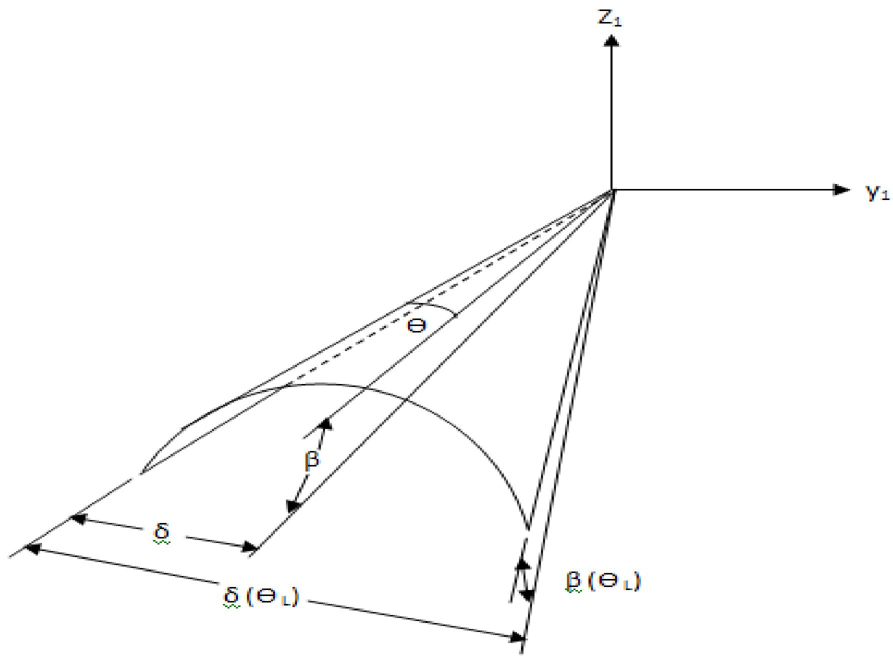

Fig 2(b): Loaded Surface of Sail

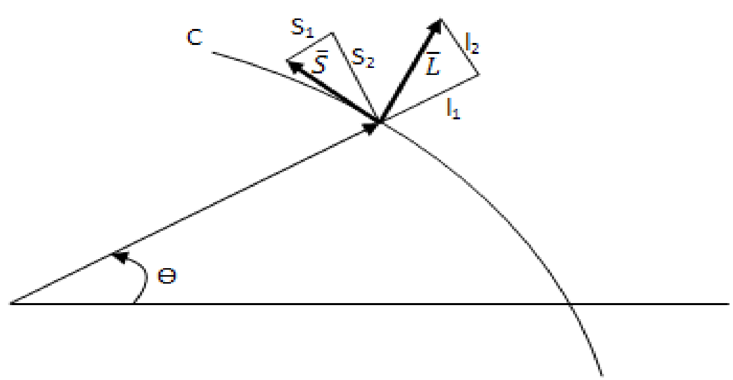

Fig. 3: Boundary Vectors

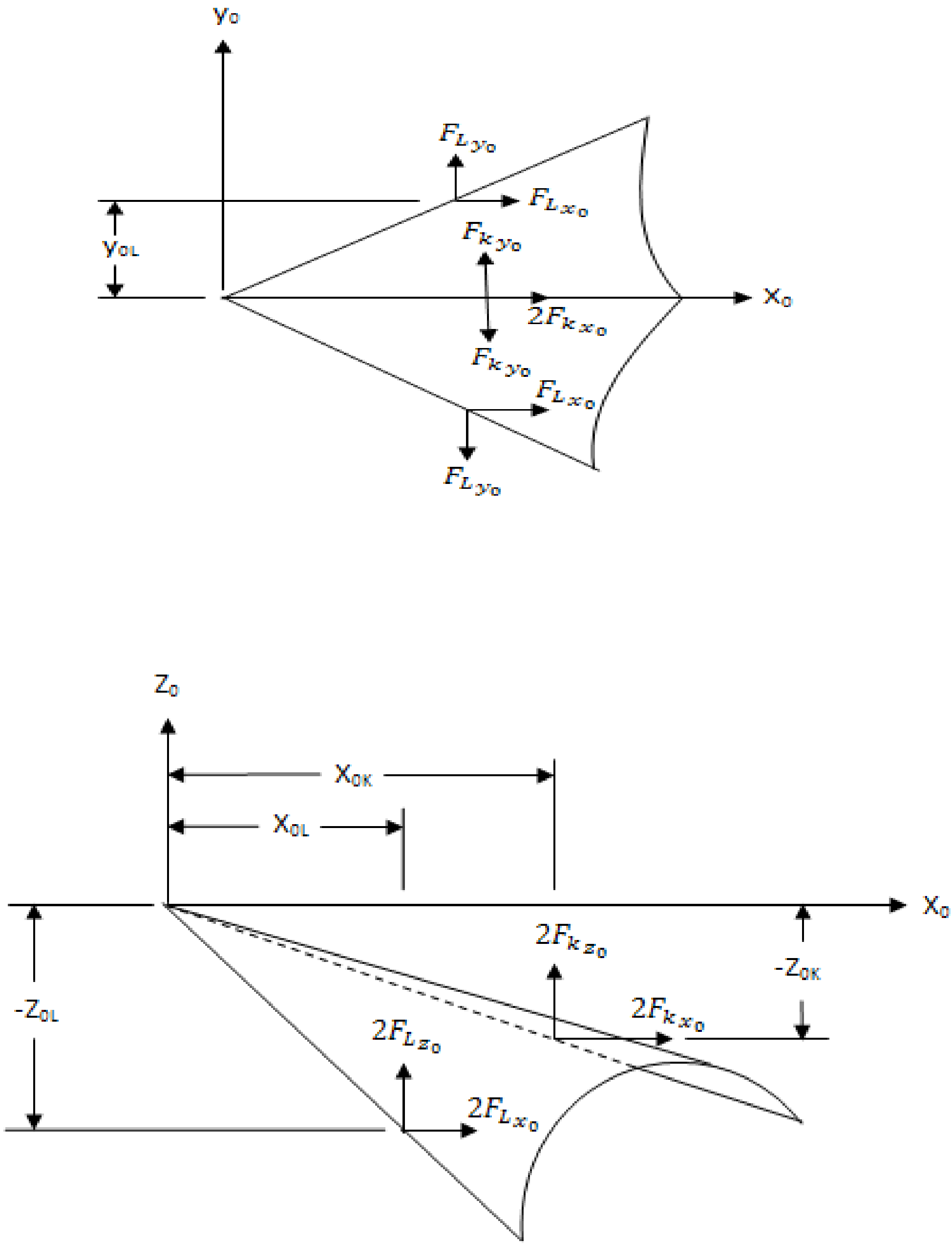

Fig. 4: Resultant forces applied by the sail to the keel and leadin-edge booms